

# Electrodeposition of Gold Nanoparticles on Electrochemically Reduced Graphene Oxide for High Performance Supercapacitor Electrode Materials

Zhihao Yu<sup>1\*</sup>, Suqin Sun<sup>2</sup> and Mingxian Huang<sup>3\*</sup>

<sup>1</sup> University of Shanghai for Science and Technology (The Public Experiment Center), NO.516 Jungong Road, Shanghai, China.

<sup>2</sup> Shanghai municipal Hospital of Traditional Chinese Medicine, NO. 274 Zhijiang mid Road, Shanghai, China.

<sup>3</sup> University of Shanghai for Science and Technology (The college of science), NO.516 Jungong Road, Shanghai, China.

E-mail: [zhihaoyuusst@gmail.com](mailto:zhihaoyuusst@gmail.com)

Received: 7 February 2016 / Accepted: 26 February 2016 / Published: 1 April 2016

---

In this contribution, reduced graphene oxide-gold nanoparticles nanocomposite (RGO-AuNPs) was synthesized using electrochemical reduction of graphene oxide (GO) at an indium tin oxide (ITO) electrode followed by an electrodeposition process of loading AuNPs on its surface. The electrochemical reduction and deposition progress were characterized by a various technique including SEM, XRD, UV-vis spectroscopy and Raman spectroscopy. The performance of RGO-AuNPs show a reversible electrochemical property and could be successfully applied as pseudocapacitor electrodes with an outstanding stability. A high specific capacity of 288 F/g at a high current density of 28 A/g was obtained in the electrochemical investigation, which shows greatly enhanced performance for supercapacitor applications.

---

**Keywords:** Reduced graphene oxide; Electrochemical; Au nanoparticles; Supercapacitor

## 1. INTRODUCTION

Supercapacitors have attracted great attentions due to their high capacitance, exceptional energy density and cycle reliability. Supercapacitors are divided into two parts with respect to charge storage mechanism; EDLC, which store charge in electrical double layer and pseudocapacitors, which are used for energy storage due to the faradic process []. Formation of polycations and loss of electrons are the key mechanism part in the charge storage in CPs. The electro neutrality of the CPs can be

maintained by the intercalation of anions into the CPs. The poor cycle life is the main problem of the CP, which caused by the accumulation of stress on polymer due to the over and over repeating the charge-discharge procedure [2]. One of the possible method for solving this problem is incorporating nanostructure materials into CPs, which could significant improvements in properties including flame retardation, electrical conductivity and thermal conductivity [3].

Graphene is a 2D material only have one layer of C atoms, which owing outstanding properties including mechanical, catalytic, thermal and electronic performances [4-9]. The high surface area of graphene make it become an excellent candidate for alternative electrode material for supercapacitors, which could result outstanding capacitance/energy density and better electronic conductivity. Therefore, the graphene can be used for increasing the power density and decline the cell resistance. The oxidation form of graphene, graphene oxide (GO) can be synthesized using low cost method and can be reduced to form reduced graphene oxide. GO can be reduced by a various methods including chemically, thermally, electrochemically and microwave-assisted techniques [5-7, 10, 11]. Recently, several reports regard the application of electrochemically reduced GO in supercapacitors were reported [12]. However, aggregation occurs upon the RGO due to their re-stacking effect, which have to be solved to remain the electrochemical performance of graphene. Loading metal nanoparticles between RGO sheets can act to expand the space between them, which make sure the remaining of large surface area and to allow electrochemical capacitance to build up on either side of the RGO [13]. Gold nanoparticles (AuNPs) are excellent material for separation of re-stacked RGO sheets [14].

In this paper, we reported the electrodeposition of AuNPs on the electrochemically RGO using GO and  $\text{HAuCl}_4$  as precursors. The entire fabrication process was conducted on a ITO electrode. The prepared RGO-AuNPs nanocomposite was then used as a good candidates for active material in supercapacitors. The cyclic voltammetry and galvanostatic charge-discharge results show that the proposed RGO-Au nanocomposite could result excellent cycling stability and rate capability in supercapacitor application.

## 2. EXPERIMENTAL

### 2.1 Materials

Graphite was used for synthesizing GO using Hummers approach [15]. Specifically, 5 g of graphite and  $\text{NaNO}_3$  were introduced into 100 mL  $\text{H}_2\text{SO}_4$  (10 M). Then,  $\text{KMnO}_4$  (10 g) was introduced into above solution under mild stirring. The mixture was kept under room temperature for half hour. Then 100 mL water was added in to the above solution and kept the solution below 100 °C for half hour. The whole reaction was ended by added 300 mL water and 20 mL  $\text{H}_2\text{O}_2$ . Centrifugation and wash process were conducted until the solution reach to pH 7. The solid product was collected and dried in an oven.  $\text{HAuCl}_4$  were were purchased from Sigma-Aldrich. All other chemicals used were analytical grade reagents without further purification

## 2.2 Electrochemical reduction of GO

ITO was used as the conductive substrate. Five milliliters GO solution (1 mg/mL) was drop coated on a ITO surface and dried under ambient conditions. GO was electrochemically reduced by CV scanning from 0.0 to  $-1.5$  V in  $N_2$ -purged 0.05 M pH 5.0 PBS for 150 cycles, and then rinsed with water and dried at room temperature.

## 2.3 Electrodeposition of AuNPs on RGO

Electrochemical deposition of AuNPs on RGO modified ITP was performed in 0.5 M  $H_2SO_4$  solution containing 1%  $HAuCl_4$  using chronoamperometry at an applied potential of  $-0.2$  V for 120s.

## 2.4 Characterization

A series of characterization techniques were used for analyzing formed material. Scanning electron microscopy (SEM, JSM 840F, Jeol) was used for observation of the surface morphology and RGO and RGO-Au NPs. Energy-dispersive X-ray spectroscopy (EDX) was used for analyzing the elemental information of formed materials. Raman spectra of the materials were taken by a Raman micro-spectrometer (Horiba Jobin-Ivon) using 514 nm laser. Surface functional groups of the prepared materials were recorded using a FTIR (Perkin-Elmer Inc., Norwalk, CT). UV-vis spectra of the samples were recorded using a UV-vis spectrometer (Shimadzu UV-1800 PC).

## 3. RESULTS AND DISCUSSION

The morphology of the RGO and RGO-Au NPs were characterized by SEM. Figure 1A-B display the typical SEM images of electrochemically reduced GO and RGO-AuNPs nanocomposite. As shown in Figure 1A, electrochemically reduced GO film displays a flake-like shape with many wrinkles. The surface of the thin film was very smooth. After chronoamperometric deposition of AuNPs (Figure 1B), the RGO sheets surface and interspace showed many deposited AuNPs. The average size of the AuNPs was calculated as 39 nm based on measuring 200 individual AuNP. The uniformity of AuNPs distribution was characterized using a high voltage SEM observation, indicating our proposed method could uniformly deposit AuNPs on the electrochemically reduced GO film without aggregation.

Figure 1C displays the EDX spectrum of RGO-AuNPs nanocomposite, which confirmed the presence of elemental C, O and Au signals. C and Au signals can be assigned to the RGO and AuNPs. O signal probably due to the existence of oxygen containing surface functional groups which have not been fully reduced using CV scans. No other impurity element was observed in the sample, indicating the high purity of the RGO-AuNPs nanocomposite. Therefore, using our proposed method for preparing RGO-AuNPs nanocomposite is a reliable method.

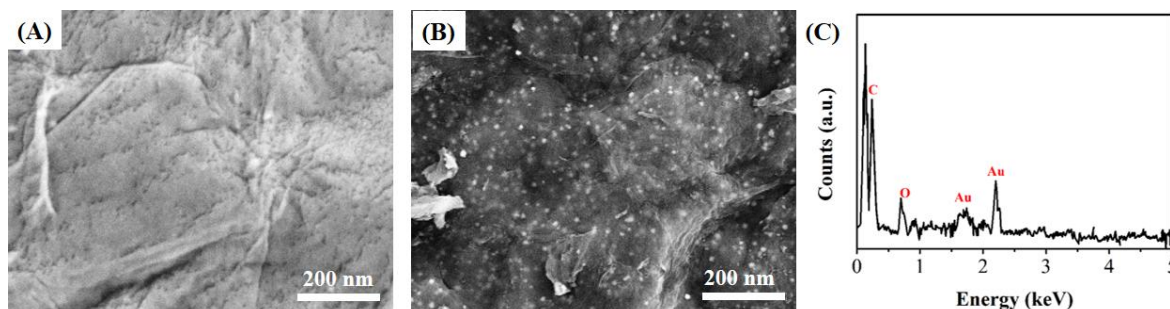


**Figure 1.** SEM images of (A) RGO and (B) RGO-AuNPs nanocomposite. (C) EDX spectrum of RGO-AuNPs nanocomposite.

The electrochemical reduction of GO need be confirmed by characterizations. Raman characterization was used for analyzing the crystal structure of GO before and after reduction. Figure 2A shows the Raman spectra of GO and RGO-AuNPs nanocomposite. As shown in figure, the Raman spectrum of GO contains D and G bands at  $1345$  and  $1592$   $\text{cm}^{-1}$ , respectively. The D band and G band can be assign to the first-order scattering of  $E_{2g}$  phonons by  $sp^2$  carbon atoms and breathing mode of  $\kappa$ -point photons of  $A_{1g}$  symmetry, respectively [16]. The intensity ratio of the D and G peaks ( $I_D/I_G$ ) increases from  $0.857$  to  $0.977$  for the RGO-AuNPs nanocomposite, indicating the  $sp^2$  domains restoration during the CV scans.

The reduction process was also confirmed by FTIR study. Typical FTIR spectra of GO and RGO are shown in Figure 2B. The strong peaks at  $3420$ ,  $1725$ ,  $1400$ ,  $1221$  and  $1068$   $\text{cm}^{-1}$  in the FTIR spectrum of GO can be assigned to the different oxygen-containing functional groups including OH, C=O, OH deformation and C–O [17]. After electrochemical reduction, the peak at  $1725$   $\text{cm}^{-1}$  was dispersed. Other oxygen-containing groups were reduced in intensities, suggesting the successful removal of large content of the oxygen-containing groups. Moreover, the peaks at  $1635$   $\text{cm}^{-1}$ ,  $2935$  and  $2860$   $\text{cm}^{-1}$  in the RGO-AuNPs can be assigned to the C=C bond and two different types of  $-\text{CH}_2$  groups, which can be used for confirming the reduction of GO [18].

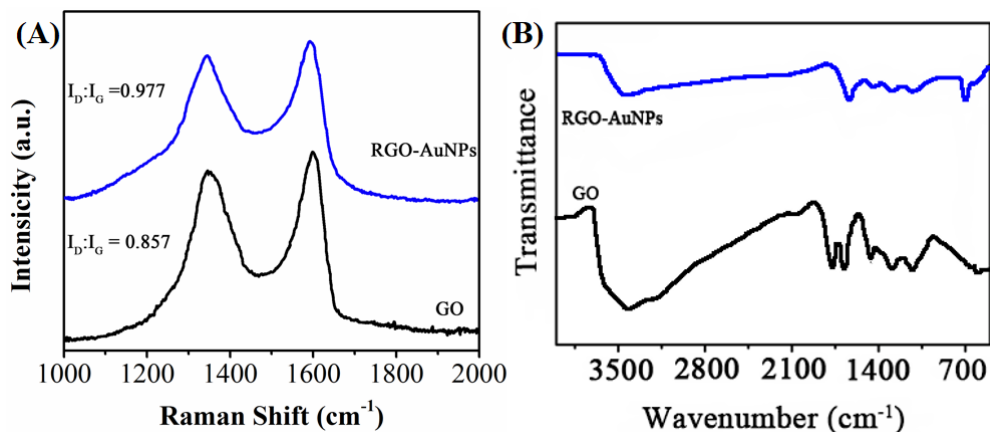


**Figure 2.** (A) Raman and (B) FTIR spectra of GO and RGO-AuNPs nanocomposite.

The reduction process was also confirmed by the UV-vis spectroscopy. As shown in the Figure 3A, the spectrum of the GO shows two characteristic peaks at 228 nm and 317 nm due to the  $\pi-\pi^*$  transitions of aromatic C—C bonds and  $n-\pi^*$  transitions of C=O bonds, respectively [19]. In contrast, the spectrum of the RGO-AuNPs shows a peak shift from 228 nm to 274 nm, further confirming the reduction of GO [20]. The formation of AuNPs under electrodeposition process was also confirmed by UV-vis spectroscopy. As shown in the Figure 3A, after deposition of AuNPs, the spectrum of the sample exhibits a new broad absorption peak centred at about 510 nm, corresponding to the surface plasmon absorption of Au nanoparticles, confirming the existence of Au nanoparticles in the sample [21].

Figure 3B shows an Au 4f XPS spectrum of RGO-AuNPs nanocomposite. The Au  $4f_{7/2}$  peak appeared at a binding energy of 84.11 eV and the Au  $4f_{5/2}$  peak appeared at a binding energy of 87.91 eV. This indicates the formation of metallic gold [22, 23].

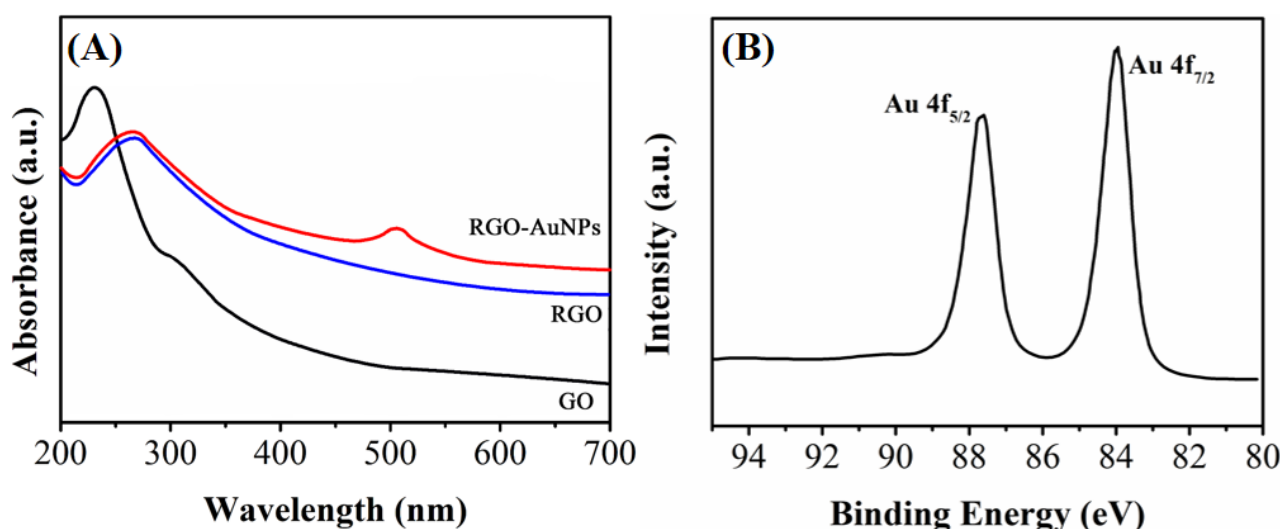


**Figure 3.** (A) UV-vis spectra of GO, RGO and RGO-AuNPs nanocomposite (B) Au 4f narrow XPS scan of the RGO-AuNPs nanocomposite.

The electrochemical property of synthesized RGO-Au nanocomposite was then evaluated by CV. Figure 4A shows the CVs of RGO and RGO-AuNPs nanocomposite modified ITO in 1 M  $H_2SO_4$  solution at the sweep rate of 25 mV/s. It can be seen that the capacitance of RGO-AuNPs nanocomposite modified ITO is about 1.5-fold larger than that of RGO modified ITO, which shows using RGO-AuNPs nanocomposite modified ITO increases the electrode capacity. The CV of RGO-AuNPs nanocomposite modified ITO shows almost symmetrical rectangular shapes, which suggests the presence of AuNPs on the RGO sheets not only increase the electrode capacitance performance, also saving its ideal capacitive behavior. Following formula was used for calculating the SC of the electrode:

$$C = \frac{I}{mv}$$

where  $I$  is the current,  $m$  is the mass of reactive material and  $\nu$  is the potential scan rate. Therefore, the RGO and RGO-AuNPs nanocomposite were calculated to be 209 and 357 F/g, respectively.

Figure 4B displays the relationship between the SC of the RGO and RGO-AuNPs nanocomposite modified ITO and scan rates. It can be seen that the SC of the RGO and RGO-AuNPs nanocomposite decreases after scan rate increasing due to the fast sweep rates leads outer porosity are use and deeper those are not accessible for doping/undoing process.

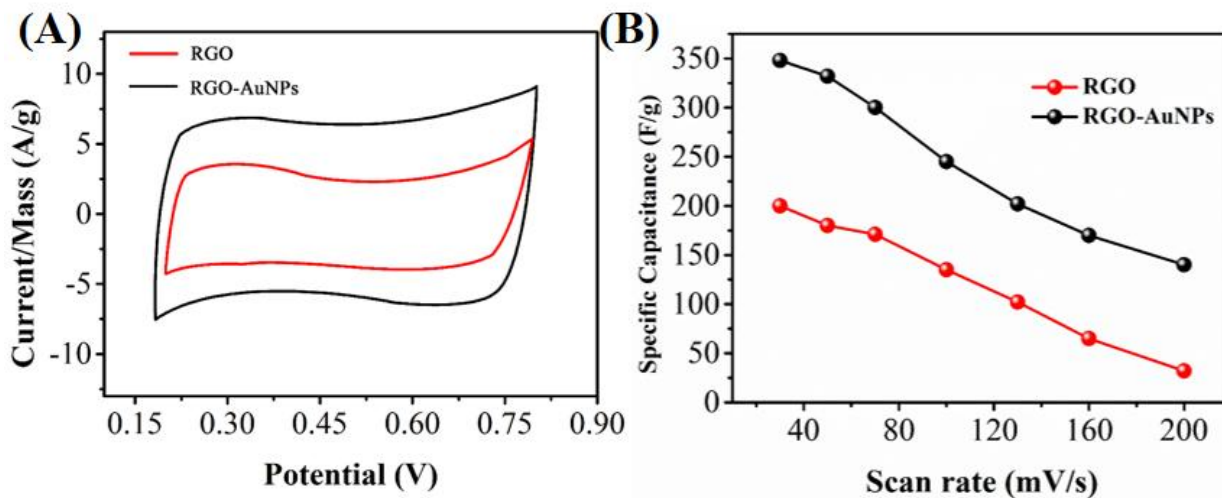


**Figure 4.** (A) Cyclic voltammograms of RGO and RGO-AuNPs nanocomposite modified ITO in 1 M H<sub>2</sub>SO<sub>4</sub> at the sweep rate of 25 mV/s in the potential window of 0.2–0.8 V. (B) Specific capacitance for RGO and RGO-AuNPs nanocomposite modified ITO in 1 M H<sub>2</sub>SO<sub>4</sub> solution using different scan rate.

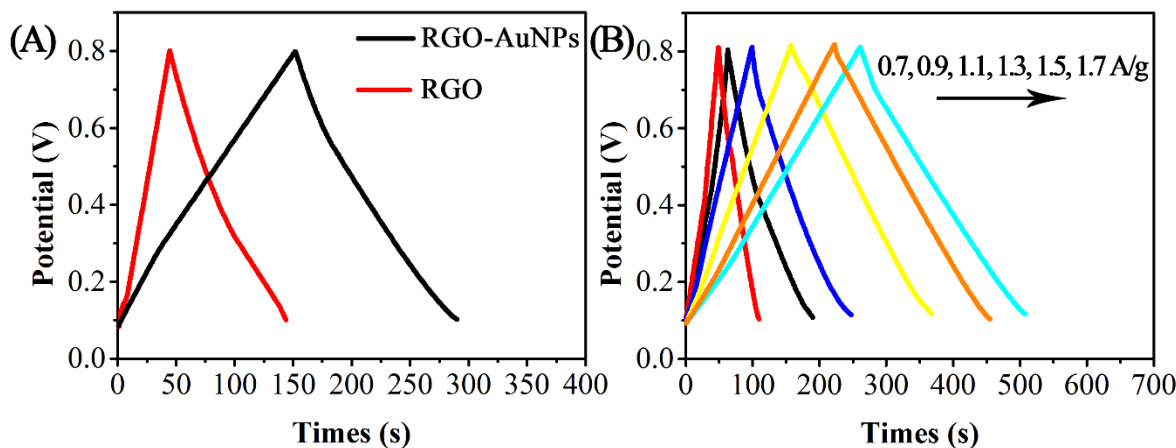


**Figure 5.** (A) Galvanostatic charge and discharge measurements of RGO and RGO-AuNPs nanocomposite modified ITO in 1 M H<sub>2</sub>SO<sub>4</sub> solution at the current density of 1.5 A/g. (B) Galvanostatic charge–discharge curves of RGO-AuNPs nanocomposite modified ITO at 0.7, 0.9, 1.1, 1.3, 1.5 and 1.7 A/g in 1 M H<sub>2</sub>SO<sub>4</sub> solution.

Galvanostatic charge/discharge approach was adopted for analyzing the capacitance of the RGO and RGO-AuNPs nanocomposite modified ITO. Figure 5A shows the charge/discharge curves of the RGO and RGO-AuNPs nanocomposite modified ITO in the potential range from 0.1 to 0.8 V at the current density of 1.5 A/g. As shown in the figure, a triangular shape between this potential range is observed that suggesting the excellent coulombic efficiency and ideal capacitive performance of the RGO-AuNPs nanocomposite modified ITO.

Figure 5B displays the charge–discharge curves of RGO-AuNPs nanocomposite modified ITO at various specific currents of 0.7, 0.9, 1.1, 1.5, 1.7 and 1.9 A/g. As shown in the figure, by enhancing the specific current, SC showed a decreasing due to the intercalation of ions at the electrode/electrolyte interface. While if low specific current was applied, the SC increased due to the enough time for ions insertion and deinsertion. These phenomena can conclude from this data that in low density currents the voltage range in charge–discharge curves decreased.

SC has been calculated by the charge/discharge curves, using following equation::

$$SC = \frac{I}{(\Delta E / \Delta t)m}$$

where  $i$  is the applied current,  $-\Delta E/\Delta t$  is the slope of the discharge curve after the voltage drop at the beginning of each discharge (ESR) and  $m$  is the mass of composite electrodes. The most SC for composite electrode is obtained when the current density for charge/discharge process is 1.1 A/g.

The cycle life of the supercapacitor as an important factor for practical applications was examined up to 1000 charge/discharge cycles. The specific capacitance of RGO-AuNPs nanocomposite modified ITO was 357 F/g in the first cycle and remained almost constant around 270 F/g from the second cycle on, indicating the excellent capacitive stability and reversibility. Comparing with other previous studies, the RGO-AuNPs nanocomposite modified ITO shows a superior performance due to its unique 2D composite structures [24-30]. The CV curves of RGO-AuNPs nanocomposite modified ITO after 1500 cycles and two week storage were also compared to estimate the retention. A very little loss in capacitance can be seen and therefore RGO-AuNPs nanocomposite is suitable for high-performance supercapacitor applications.

#### 4. CONCLUSION

In summary, RGO-AuNPs nanocomposite was prepared by electrochemical reduction of GO at an ITO electrode followed by an electrodeposition process of loading AuNPs on its surface. The synthesized RGO-AuNPs nanocomposite was characterized by SEM, Raman spectroscopy, UV-vis spectroscopy and XPS, and then employed successfully applied for supercapacitive application. Results show that RGO-AuNPs nanocomposite modified ITO has a good effect on the pseudo capacitive behavior of RGO modified ITO. The specific capacitance of RGO-AuNPs nanocomposite modified ITO is much higher than RGO modified ITO. Moreover, the stability test showed that the proposed composite has a long-term applications in high-performance supercapacitors.

**Reference**

1. J. Shabani Shayeh, A. Ehsani, M.R. Ganjali, P. Norouzi and B. Jaleh, *Appl. Surf. Sci.*, 353 (2015) 594
2. M.E. Roberts, D.R. Wheeler, B.B. McKenzie and B.C. Bunker, *Journal of Materials Chemistry*, 19 (2009) 6977
3. B.P. Grady, A. Paul, J.E. Peters and W.T. Ford, *Macromolecules*, 42 (2009) 6152
4. W. Li and Y.J. Yang, *Journal of Solid State Electrochemistry*, 18 (2014) 1621
5. Y. Zheng, A. Wang, H. Lin, L. Fu and W. Cai, *RSC Advances*, 5 (2015) 15425
6. S. Xu, L. Fu, T.S.H. Pham, A. Yu, F. Han and L. Chen, *Ceram. Int.*, 41 (2015) 4007
7. F. Han, H. Li, J. Yang, X. Cai and L. Fu, *Physica. E*, 77 (2016) 122
8. L. Fu, Y.-H. Zheng and Z.-X. Fu, *Chemical Papers*, 69 (2015) 655
9. L. Fu, Y. Zheng, A. Wang, W. Cai and H. Lin, *Food chemistry*, 181 (2015) 127
10. J. Yang and S. Gunasekaran, *Carbon*, 51 (2013) 36
11. L. Fu, D. Zhu and A. Yu, *Spectrochimica Acta Part A: Molecular and Biomolecular Spectroscopy*, 149 (2015) 396
12. A. Sun, J. Zheng and Q. Sheng, *Electrochimica Acta*, 65 (2012) 64
13. C.L. Scott and M. Pumera, *Electroanalysis*, 23 (2011) 858
14. F. Gunes, H.-J. Shin, C. Biswas, G.H. Han, E.S. Kim, S.J. Chae, J.-Y. Choi and Y.H. Lee, *ACS nano*, 4 (2010) 4595
15. W.S. Hummers and R.E. Offeman, *Journal of the American Chemical Society*, 80 (1958) 1339
16. Z.-J. Fan, W. Kai, J. Yan, T. Wei, L.-J. Zhi, J. Feng, Y.-m. Ren, L.-P. Song and F. Wei, *ACS Nano*, 5 (2010) 191
17. J. Zhang, H. Yang, G. Shen, P. Cheng, J. Zhang and S. Guo, *Chemical Communications*, 46 (2010) 1112
18. S. Bose, T. Kuila, A.K. Mishra, N.H. Kim and J.H. Lee, *Journal of Materials Chemistry*, 22 (2012) 9696
19. J.I. Paredes, S. Villar-Rodil, A. Martínez-Alonso and J.M.D. Tascón, *Langmuir*, 24 (2008) 10560
20. D. Li, M.B. Muller, S. Gilje, R.B. Kaner and G.G. Wallace, *Nat Nano*, 3 (2008) 101
21. Y. Zheng, A. Wang, H. Lin, L. Fu and W. Cai, *RSC Advances*, 5 (2015) 15425
22. M. Seah, G. Smith and M. Anthony, *Surface and interface analysis*, 15 (1990) 293
23. T.D. Thomas and P. Weightman, *Physical Review B*, 33 (1986) 5406
24. Z. Lin, X. Yan, J. Lang, R. Wang and L.-B. Kong, *Journal of Power Sources*, 279 (2015) 358
25. M. Zhou, Y. Deng, K. Liang, X. Liu, B. Wei and W. Hu, *Journal of Electroanalytical Chemistry*, 742 (2015) 1
26. D.F. Zeigler, S.L. Candelaria, K.A. Mazzio, T.R. Martin, E. Uchaker, S.-L. Suraru, L.J. Kang, G. Cao and C.K. Luscombe, *Macromolecules*, 48 (2015) 5196
27. B.C. Kim, H.T. Jeong, C.J. Raj, Y.-R. Kim, B.-B. Cho and K.H. Yu, *Synthetic Metals*, 207 (2015) 116
28. M. Luo, Y. Dou, H. Kang, Y. Ma, X. Ding, B. Liang, B. Ma and L. Li, *Journal of Solid State Electrochemistry*, 19 (2015) 1621
29. S. Mandal, A. Pal, R.K. Arun and N. Chanda, *Journal of Electroanalytical Chemistry*, 755 (2015) 22
30. T. Adinaveen, L.J. Kennedy, J.J. Vijaya and G. Sekaran, *Journal of Material Cycles and Waste Management*, 17 (2015) 736